ISSN 0036-0236, Russian Journal of Inorganic Chemistry, 2022, Vol. 67, No. 6, pp. 830–838. © Pleiades Publishing, Ltd., 2022.
Russian Text © The Author(s), 2022, published in Zhurnal Neorganicheskoi Khimii, 2022, Vol. 67, No. 6, pp. 761–769.

SYNTHESIS AND PROPERTIES OF INORGANIC COMPOUNDS

Formation of $ZrTiO_4$ under Hydrothermal Conditions

A. K. Bachina[a], *, O. V. Almjasheva[b], and V. I. Popkov[a]

[a] *Ioffe Institute, Russian Academy of Sciences, St. Petersburg, 194021 Russia*
[b] *Saint Petersburg Electrotechnical University "LETI," St. Petersburg, 197376 Russia*
**e-mail: a.k.bachina@gmail.com*

Received November 10, 2021; revised November 24, 2021; accepted November 30, 2021

Abstract—The formation of nanocrystals in the ZrO_2–TiO_2–H_2O system during isothermal (240°C) treatment of coprecipitated hydroxides under hydrothermal conditions has been studied. The formation of solid solutions based on monoclinic ZrO_2, anatase (TiO_2), and a high-temperature disordered phase of variable composition $Zr_xTi_{(1-x)}O_4$ with a scrutinyite (α-PbO_2) structure has been demonstrated. The average size of $Zr_xTi_{(1-x)}O_4$ crystallites is 16 ± 2 nm. The kinetic features of phase formation in the ZrO_2–TiO_2–H_2O system have been studied. It has been shown that the phase of variable composition $Zr_xTi_{(1-x)}O_4$ is metastable and, with increasing hydrothermal treatment duration, decomposes into solid solutions based on monoclinic ZrO_2 and anatase.

Keywords: coprecipitation, nanocrystals, $ZrTiO_4$, hydrothermal synthesis
DOI: 10.1134/S003602362206002X

The ZrO_2–TiO_2 system is actively studied because of the large number of applications for materials based on it [1–7]. Of interest are also well-studied individual components of the system in the form of various polymorphs: titanium dioxide with an anatase (*a*-TiO_2), rutile (*r*-TiO_2), and brookite (*b*-TiO_2) structure, as well as cubic, tetragonal, and monoclinic zirconia (*c*-ZrO_2, *t*-ZrO_2, and *m*-ZrO_2, respectively). The results of the practical application of composites of these phases and solid solutions based on them have been reported [8–12]. Much attention is paid to ordered and disordered zirconium titanate polymorphs, which are of interest from both fundamental and practical points of view. From a fundamental point of view, the structural and thermodynamic features of their formation are of interest [13–19] and from a practical point of view, the dielectric properties of ceramic materials based on zirconium titanate [20–22].

At present, the existence of four polymorphs of a variable-composition $Zr_xTi_{(1-x)}O_4$ phase is known. The structure of three of them is described by an orthorhombic system (space group *Pbcn*), and one polymorph is monoclinic (space group *C*12/*c*1). The orthorhombic ones include the high-temperature disordered modification of $ZrTiO_4$ with the scrutinyite (α-PbO_2) structure and low-temperature modifications that have undergone ordering of cationic octahedra with a columbite/fersmite structure, as well as the $(Zr,Ti)_2O_4$ phase with a narrow temperature range of existence from 1160 to 1060°C [14, 17, 18, 23–27]. The poorly studied compound $Zr_{1.34}Ti_{0.66}O_4$ with a fergusonite structure is attributed to monoclinic [28].

The possibility of formation of a certain modification of $Zr_xTi_{(1-x)}O_4$ largely depends on the synthesis method and conditions. There are data in the literature on the high-temperature region of the phase diagram of the ZrO_2–TiO_2 system and methods for fabricating materials based on disordered zirconium titanate [15, 18, 20, 23, 29, 30]. There are much fewer data on the low-temperature region of the ZrO_2–TiO_2 phase diagram, and they often contradict each other [14, 17, 24]. However, it has been shown that ceramics based on ordered low-temperature modifications of zirconium titanate have higher dielectric properties, which deteriorate in the presence of the ZrO_2 impurity [21].

Hydrothermal synthesis is a "soft chemistry" method that successfully produces nanocrystalline oxide materials with a narrow particle size distribution [31]. Reducing the synthesis temperature compared to conventional heat treatment methods becomes possible due to the partial dissolution of the reagents in a hydrothermal fluid at elevated pressure, which reduces diffusion limitations and increases the mass transfer rate in the system. This, in turn, leads to a faster achievement of the equilibrium state in the system [31].

In view of the foregoing, this study focuses on determining the features of the formation of the crystal structure and the stability of zirconium titanate and other components of the ZrO_2–TiO_2 system under hydrothermal conditions.

EXPERIMENTAL

The starting reagents were $ZrOCl_2 \cdot 8H_2O$ (reagent grade, TU 6-09-3677-74), $TiCl_4$ (reagent grade TU 6-09-2118-77), 25% aqueous NH_4OH (State Standard GOST 24147-80), and distilled water State Standard GOST 6709-72).

Samples for study were obtained by coprecipitation from aqueous solutions of zirconyl chloride ($ZrOCl_2$) and hexachlorotitanic acid (H_2TiCl_6) with aqueous ammonia (NH_4OH) to pH 10. H_2TiCl_6 was synthesized from titanium tetrachloride ($TiCl_4$) by the procedure described in [32]. The $ZrOCl_2$-to-H_2TiCl_6 ratio was selected to prepare $Zr_xTi_{(1-x)}O_2$ compositions with x = 1.0, 0.95, 0.85, 0.75, 0.65, 0.55, 0.45, 0.35, 0.15, 0.05, and 0.0 by the following chemical reaction:

$$x\mathrm{ZrOCl_2} + (1-x)\,\mathrm{H_2TiCl_6} + (6-4x)\,\mathrm{NH_4OH} \rightarrow \mathrm{Zr_xTi_{(1-x)}O_2} + (6-4x)\,\mathrm{NH_4Cl} + (4-3x)\,\mathrm{H_2O}.$$

The precipitates were washed with distilled water until it showed a negative reaction to chloride ion, and dried at 95°C in air. In this way, eleven starting compositions were synthesized; they were denoted as ZT100, ZT95, ZT85, ZT75, ZT65, ZT55, ZT45, ZT35, ZT15, ZT5, and ZT0 and corresponded to $Zr_xTi_{(1-x)}O_2$ at x = 1.0, 0.95, 0.85, 0.75, 0.65, 0.55, 0.45, 0.35, 0.15, 0.05, and 0.0, respectively.

The resulting compositions were subjected to hydrothermal treatment at 240°C and 70 MPa in 16-cm^3 Teflon-lined autoclaves. Distilled water was used as the hydrothermal medium. The duration of isothermal treatment varied from 4 to 48 h. After the end of isothermal treatment and complete cooling of the autoclaves, the samples were taken out and dried at 100°C.

The chemical composition of the samples was determined by energy dispersive X-ray microanalysis (EDXMA) on a Hitachi S-570 scanning electron microscope equipped with a Bruker Quantax 200 microprobe system. The error in determining the content of elements by this method is, on average, ±0.3 wt %.

For the X-ray diffraction (XRD) study, a Shimadzu XRD 7000 diffractometer with CuK_α radiation (λ = 1.54056 Å) was used. Reflection intensity data were collected in the range 2θ angles from 5° to 100°. The X-ray powder diffraction method was used. To identify the phases, the recorded X-ray diffraction patterns were compared with the structural data of inorganic substances from the ICSD database. The quantitative phase composition and size of crystallites (coherent scattering regions) were determined using the Rietveld full profile analysis method; the fraction of the amorphous phase was determined using an internal standard, silicon powder (SRM 640f, NIST). The crystallite size was calculated from the broadening of X-ray diffraction lines using the Scherrer formula. All calculations were performed using the PDWin 4.0 software package.

Differential thermal analysis was performed on a Netzsch STA 449F3 instrument. The measurements were carried out in the temperature range 25–1200°C in an argon flow (20 mL/min) at a rate of 10 K/min.

RESULTS AND DISCUSSION

Initial Composition

The EDXMA method confirmed the absence of chemical impurities in the starting compositions. Figure 1a shows the energy dispersive X-ray spectrum, which shows that sample ZT45 contains three major elements: titanium Ti, zirconium Zr, and oxygen O. The characteristic lines of aluminum Al and carbon C in the spectrum are a consequence of sample preparation and imaging procedures. Similar spectra were obtained for all samples, in which the presence of impurities was also not observed. According to EDXMA, the content of the elements in the initial samples in terms of simple oxides (ZrO_2 and TiO_2) was in good agreement with the composition specified for the synthesis; the maximum deviation did not exceed 3 mol % (Fig. 1b). All starting samples were X-ray amorphous. Figure 1c shows the X-ray diffraction pattern of sample ZT45 as an example. Similar diffraction patterns, characteristic of X-ray amorphous substances, were obtained for all initial samples of coprecipitated hydroxides.

Simple Oxides ZrO_2 and TiO_2 and Solid Solutions Based on Them

Figure 2 shows the X-ray diffraction patterns in the range of 2θ angles corresponding to the most intense peaks of possible crystalline phases in the ZrO_2–TiO_2 system. According to XRD data, hydrothermal treatment of individual zirconium and titanium hydroxides for 4 h yielded a mixture of monoclinic and tetragonal ZrO_2 crystalline phases in a ratio of 35 : 65 mol % in the case of sample ZT100 and anatase TiO_2 in the case of sample ZT0 (Fig. 2a). The results obtained are in good agreement with the data of [32–35]. In both cases, the average size of ZrO_2 and TiO_2 nanocrystals is ~15 ± 2 nm.

An increase in the duration of isothermal hydrothermal treatment of simple hydroxides to 24 h leads to an insignificant increase in the average size of crystallites, and the phase composition does not undergo noticeable changes (Fig. 2b). According to XRD data, the phase composition in the ZrO_2–H_2O system does not change; in the TiO_2–H_2O system, the appearance of small amounts of brookite is observed.

In the ZrO_2–TiO_2–H_2O system in the range of low (up to 5 mol %) TiO_2 content (sample ZT95), the X-ray diffraction pattern shows only the peaks of *m*-ZrO_2 and *t*-ZrO_2. In this case, a shift of reflections relative to pure ZrO_2 is observed. The unit cell param-

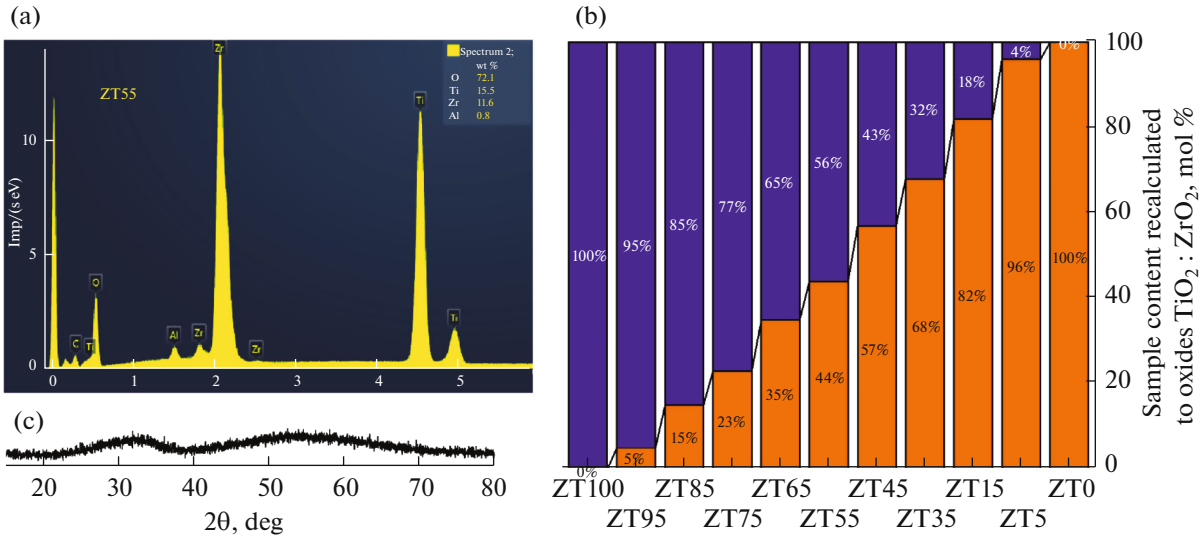

Fig. 1. (a) EDX spectrum of sample ZT55; (b) the content of the samples recalculated to oxides according to EDXMA data: (blue) ZrO_2 and (orange) TiO_2; (c) X-ray powder diffraction patterns of sample ZT55 before hydrothermal treatment.

eters of *m*-ZrO_2 have been refined by the Rietveld method. Figure 3b shows that the unit cell volume of *m*-ZrO_2 decreases with an increase in the TiO_2 content in the system, which indicates the formation of ZrO_2 solid solutions based on the monoclinic (*m*-ZrO_2(sol. sol.)) modification. The average crystallite size of both crystalline phases decreases compared to pure ZrO_2 to 13 ± 5 nm. No quantitative redistribution of phases is observed. An increase in the of isothermal treatment duration to 24 h does not lead to significant changes in the diffraction pattern (Fig. 2).

For the samples with an excess of zirconium (ZT85, ZT75, ZT65), after hydrothermal treatment for 4 h, weak reflections in the range of (100) peaks of *m*-ZrO_2, *t*-ZrO_2, and $Zr_xTi_{(1-x)}O_4$ are fixed in the diffraction patterns against the background of an amorphous halo. This behavior of the system can be explained by the fact that, similarly to zirconium hydroxide, in the simple ZrO_2–H_2O system [35, 36], complex amorphous zirconium hydroxide with titanium included in its structure was formed at the coprecipitation stage, and its dehydration followed by crystallization requires other synthesis conditions.

With an increase in the duration of isothermal treatment, crystallization of *t*-ZrO_2(sol. sol.) and m-ZrO_2(sol. sol.) occurs in samples ZT85 and ZT75, as evidenced by a pronounced shift of reflections in the diffraction patterns (Fig. 2a). The fraction of *m*-ZrO_2(sol. sol.) sharply increases (Fig. 3a). In particular, only a trace amount of *t*-ZrO_2(sol. sol.) is fixed in the ZT75 sample. Reflections corresponding to crystalline modifications of TiO_2 are not observed in any of these samples.

According to [17], in the ZrO_2–TiO_2 system, the $Zr_xTi_{(1-x)}O_4$ compound is formed within the TiO_2 concentration range from 34 to 75 mol %. In the present work, in sample ZT65, corresponding to a TiO_2 content of 35 mol %, after hydrothermal treatment for 24 h, X-ray diffraction revealed reflections of the high-temperature disordered modification of $Zr_xTi_{(1-x)}O_4$ with an α-PbO_2 structure. Along with the peaks of the compound, the diffraction pattern contains peaks of *m*-ZrO_2(sol. sol.), while the reflections corresponding to the crystalline modifications of TiO_2 are not observed.

With an increase in the TiO_2 content in the ZrO_2–TiO_2–H_2O system up to 45 mol % (sample ZT55), hydrothermal treatment for 4 h does not lead to crystallization of any phases, and the sample remains X-ray amorphous. With an increase in the duration of hydrothermal treatment to 24 h, crystallization of $Zr_xTi_{(1-x)}O_4$ and *m*-ZrO_2(sol. sol.) occurs in a ratio close to 1 : 1.

In the ZrO_2–TiO_2–H_2O system in the range of low (from 5 to 45 mol %) ZrO_2 concentrations (samples ZT5, ZT15, ZT35, and ZT45), hydrothermal treatment for 4 h yielded TiO_2 nanocrystals with the anatase structure (Fig. 2). The shift of the anatase peaks in the diffraction patterns with an increase in the ZrO_2 content suggests that zirconium enters the structure of anatase, forming a solid solution based on it (*a*-TiO_2(sol. sol.)), which is also evidenced by a change in the unit cell parameters (Fig. 3d). In addition to the anatase-based solid solution, the diffraction patterns show a weak reflection in the range of 100% peaks of $Zr_xTi_{(1-x)}O_4$, *t*-ZrO_2, and the (211) brookite reflection. It is known that the solubility limit of ZrO_2 in

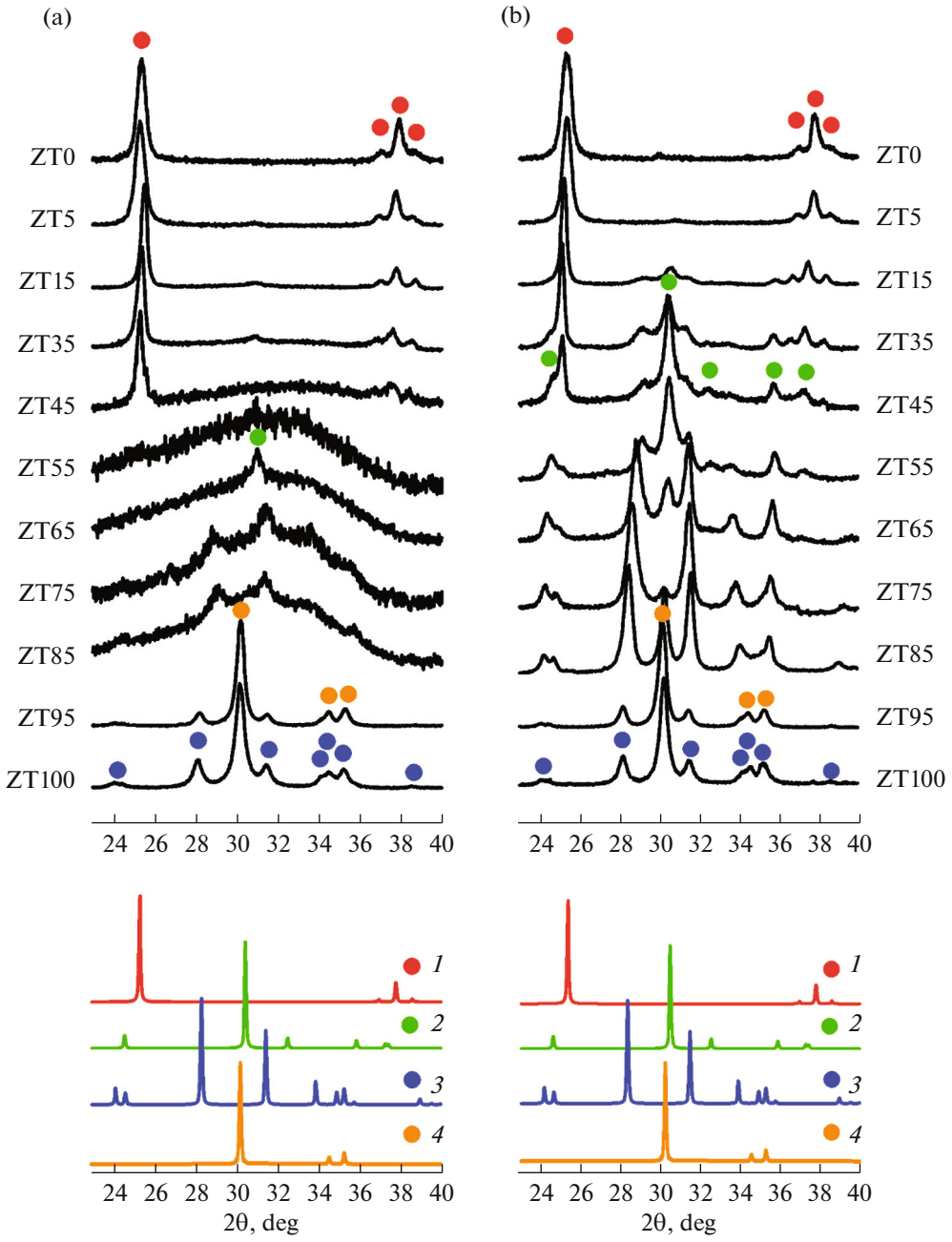

Fig. 2. X-ray powder diffraction patterns of samples after hydrothermal treatment at 240°C for (a) 4 and (b) 24 h. X-ray powder diffraction patterns of (*1*) anatase, (*2*) zirconium titanate, (*3*) monoclinic zirconium dioxide, and (*4*) tetragonal zirconium dioxide from the ICSD database (nos. 82082, 51049, 68782, and 68781, respectively).

TiO_2 is relatively low and, according to [17, 23, 37], does not exceed 18 mol %. Therefore, it can be assumed that part of the zirconium that did not enter the anatase structure remained in the form of an amorphous hydroxide.

An increase in the duration of isothermal treatment to 24 h leads to the crystallization of $Zr_xTi_{(1-x)}O_4$ and *m*-ZrO_2(sol. sol.) in samples ZT15, ZT35, and ZT45. From the X-ray diffraction pattern corresponding to the ZT5 sample, the Rietveld method demonstrated the formation of a mixture of *a*-TiO_2(sol. sol.) and brookite (*b*-TiO_2) phases, while no zirconium-containing phases were detected (Figs. 2 and 3a, 3c).

Figure 3c shows how the average size of ZrO_2 and TiO_2 crystallites changes during the formation of solid solutions depending on the concentration of the components. The average crystallite size of the ZrO_2 solid solution based on the monoclinic modification

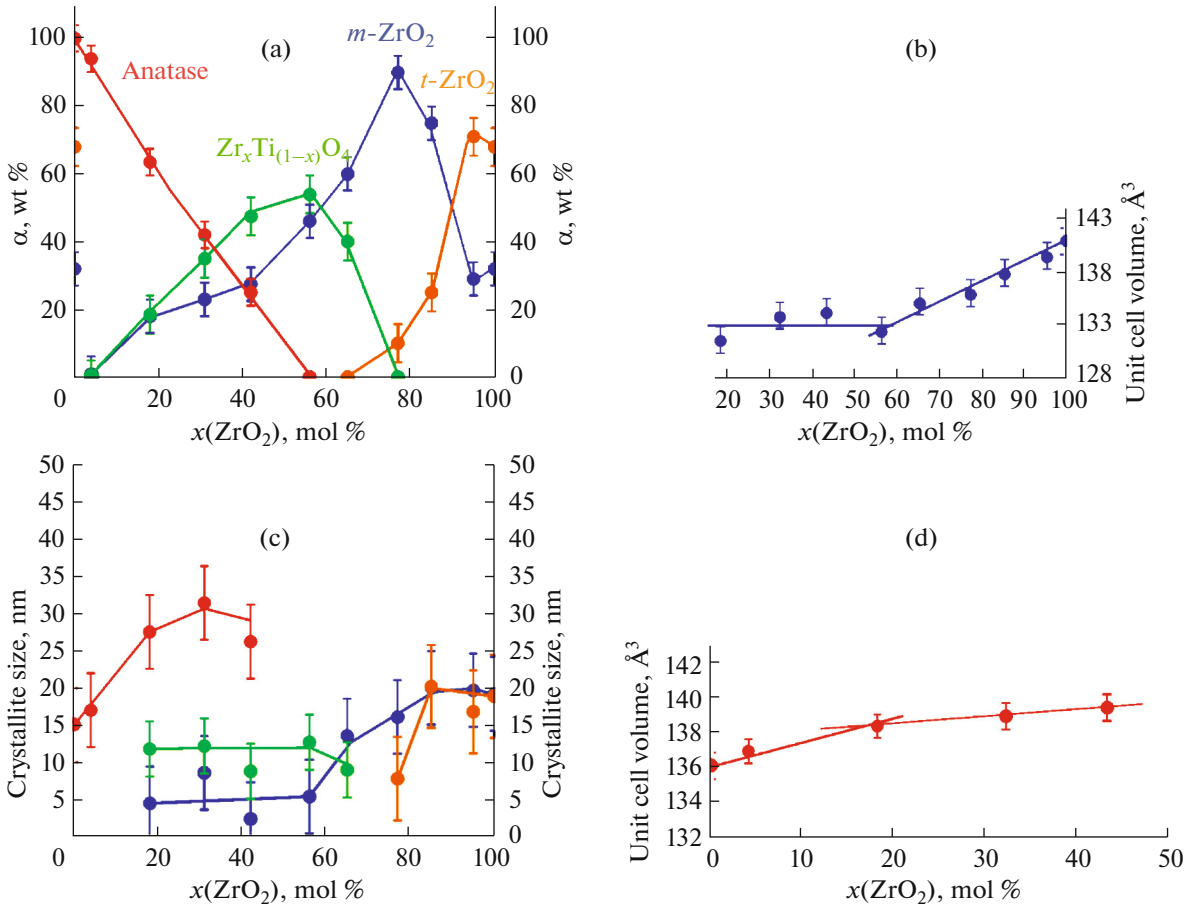

Fig. 3. Changes in the (a) phase composition and (c) crystallite size of the samples after hydrothermal treatment for 24 h depending on the ZrO_2 content in the ZrO_2–TiO_2 system. Changes in the unit cell volume of (b) monoclinic ZrO_2 and (d) anatase depending on the ZrO_2 content in the ZrO_2–TiO_2 system.

sharply decreases with an increase in the TiO_2 content in the system up to 44 mol % (from 18 ± 5 to 5 ± 3 nm) and then roughly does not change up to 82 mol % TiO_2, while the average size of the crystallites of the solid solution with an anatase structure increases monotonically with an increase in the fraction of ZrO_2 in the system.

Formation of the $Zr_xTi_{(1-x)}O_4$ Compound under Hydrothermal Conditions

As was shown above, the $Zr_xTi_{(1-x)}O_4$ phase does not form after hydrothermal treatment for 4 h, while individual oxides crystallize under these conditions very quickly. It is possible that at the stage of coprecipitation of titanium and zirconium salts, a double hydroxide is formed, which is a structural precursor of one of the intermediate compounds in the ZrO_2–TiO_2 system. Figure 4 shows the DTA curves obtained for the starting amorphous samples ZT100, ZT65, ZT55, ZT45, ZT35, and ZT0. These data demonstrate that the exotherms associated with the crystallization of pure oxides are observed at lower temperatures than the exotherms associated with the crystallization of the $Zr_xTi_{(1-x)}O_4$ compound. Such a pronounced difference in crystallization temperatures allows us to conclude that in the preparation of compositions ZT65, ZT55, ZT45, and ZT35, one of the coprecipitation products is a double hydroxide structurally different from pure titanium and zirconium hydroxides. The above assumptions are consistent with the data of [27, 32, 36, 38–42], where the formation of amorphous titanium and zirconium hydroxides, which are structural precursors of the crystalline ZrO_2 and TiO_2, phases has been shown under similar conditions, and the crystallization temperature of the amorphous precursors of ZrO_2, TiO_2, and $ZrTiO_4$ has been determined.

Crystallization of the $Zr_xTi_{(1-x)}O_4$ compound occurs in samples with titanium content from 35 to 82 mol % after isothermal treatment for 24 h (Figs. 2, 3a, 3c). XRD demonstrates that this phase corresponds to the structure of the high-temperature disordered $ZrTiO_4$ phase with a structure of scrutinyite

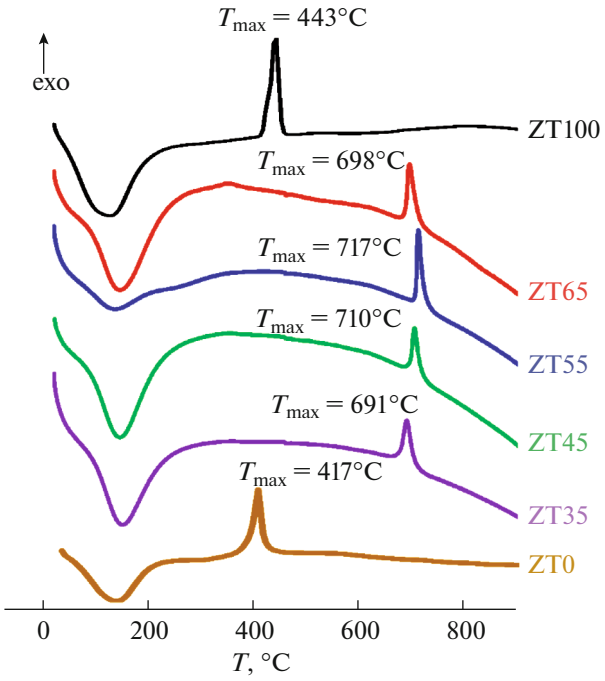

Fig. 4. DTA curves of initial amorphous samples recorded at a heating rate of 10 K/min in an argon atmosphere.

(α-PbO2). The average crystallite size of the resulting phase is within (8–12) ± 5 nm.

The Rietveld method was used to refine the crystal lattice parameters of $ZrTiO_4$. As a model for refinement, we used the structural data of card no. 153941 of the ICSD database. The refined parameters of samples ZT35, ZT45, ZT55, ZT65 and the reference sample are given in Table 1.

It has been shown [23] that, with an increase in ordering in the ZrO_2–TiO_2 system, the parameter *b* of the crystal lattice noticeably decreases. As can be seen from Table. 1, there is no decrease in the *b* parameter in samples ZT35, ZT45, ZT55 and ZT65 compared to the reference value; however, the crystal lattice parameters are slightly different. Thus, we can conclude that the compound obtained by hydrothermal treatment of coprecipitated hydroxides is a high-temperature metastable phase of variable composition $Zr_xTi_{(1-x)}O_4$ with a disordered α-PbO_2 structure. Refinement of the cationic composition of the obtained phase required additional study and was not carried out in the framework of this work.

Stability of Variable-Composition Phase $Zr_xTi_{(1-x)}O_4$ with an α-PbO_2 Structure

As follows from the X-ray powder diffraction patterns in Fig. 2b, all samples are mixtures of two or more phases, and $Zr_xTi_{(1-x)}O_4$ is always observed in the presence of the *m*-ZrO_2(sol. sol.) phase. In this regard, the kinetic dependences of phase transformations in the ZrO_2–TiO_2–H_2O system have been studied. As an illustration of the kinetics of phase transformations in the ZrO_2–TiO_2–H_2O system, Fig. 5, using sample ZT45 as an example, shows the change in the diffraction pattern depending on the duration of hydrothermal treatment and the results of XRD analysis.

Recall that initially sample ZT45 was X-ray amorphous. After hydrothermal treatment for 2 h, the corresponding diffraction pattern did not show the presence of crystalline phases. However, already 4 h of isothermal treatment led to the appearance of reflections characteristic of the *a*-TiO_2(sol. sol.) phase. Quantitatively, the content of *a*-TiO_2(sol. sol.) was ~10 wt %, and the average crystallite size was about 22 nm.

After 6 and 8 h of hydrothermal treatment, a weak reflection appears in the diffraction patterns in the range of the strongest $Zr_xTi_{(1-x)}O_4$ peak, corresponding to a small amount of this compound (Fig. 5a).

The contents of *a*-TiO_2(sol. sol.) and the amorphous phase vary slightly up to 12 h of hydrothermal treatment (Fig. 5b). In this case, the average size of *a*-TiO_2(sol. sol.) crystallites increases to 25 ± 5 nm (Fig. 5c). The content of $Zr_xTi_{(1-x)}O_4$ increases to ~8 wt %. The average size of crystallites of this phase practically does not change with an increase in the duration of isothermal treatment and is about 16 ± 2 nm.

Increasing the duration of isothermal treatment up to 24 h leads to the appearance of *m*-ZrO_2(sol. sol.) peaks in the diffraction pattern. In this case, the entire amorphous phase has already been consumed, and the process of crystallization from an amorphous substance can be considered completed. A sharp increase

Table 1. Refined unit cell parameters of the variable-composition phase $Zr_xTi_{(1-x)}O_4$ with an α-PbO_2 structure (space group *Pbcn*) and reference unit cell parameters of the (ICSD-153941)

Sample	*a*, Å	*b*, Å	*c*, Å	*V*, Å^3
ZT35	4.81 ± 0.02	5.47 ± 0.02	5.03 ± 0.02	132.27 ± 0.05
ZT45	4.81 ± 0.02	5.48 ± 0.02	5.01 ± 0.02	132.07 ± 0.05
ZT55	4.79 ± 0.02	5.51 ± 0.02	5.02 ± 0.02	132.45 ± 0.05
ZT65	4.81 ± 0.02	5.50 ± 0.02	5.02 ± 0.02	132.77 ± 0.05
ICSD-153941	4.8069	5.4785	5.0339	132.57

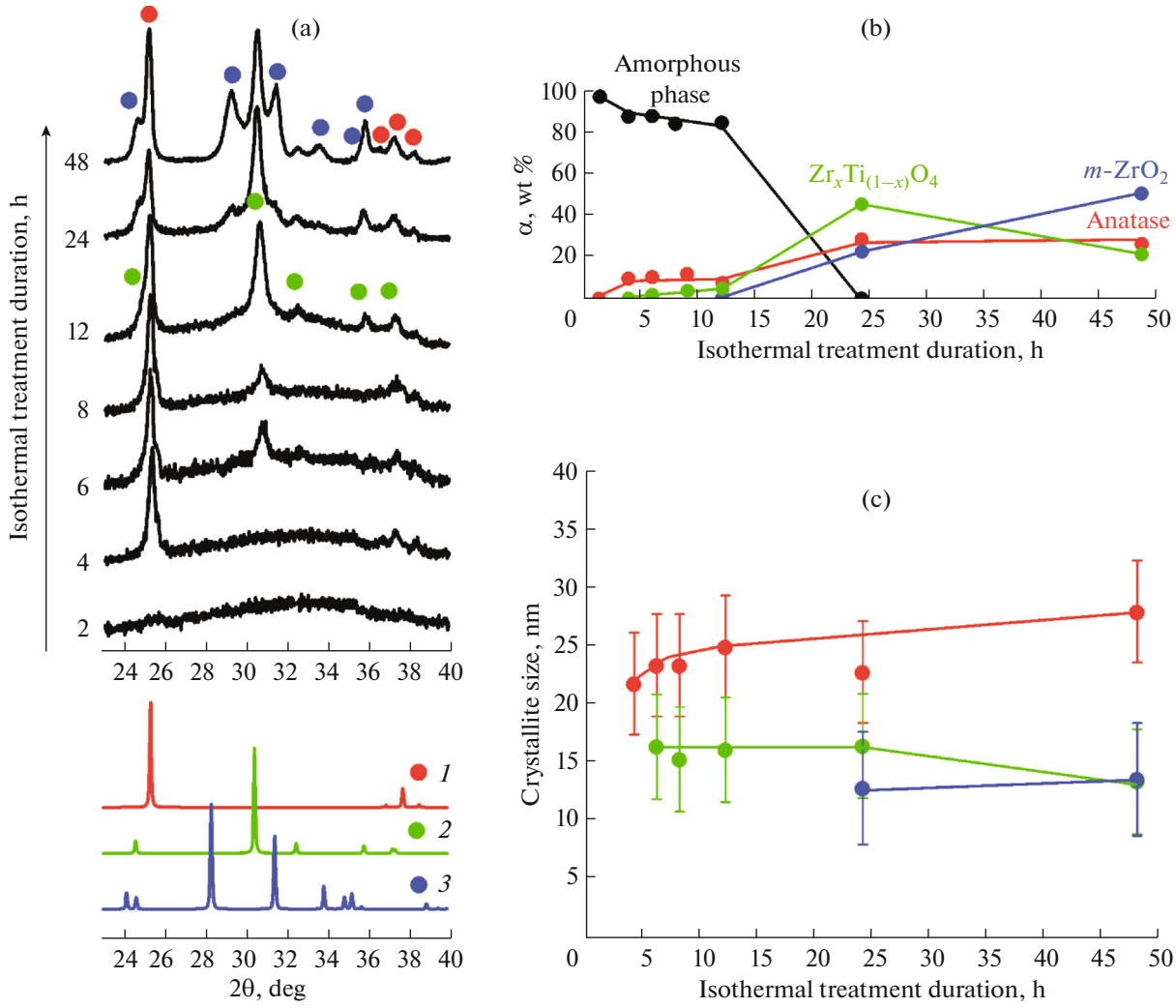

Fig. 5. X-ray powder diffraction patterns of (a) sample ZT45 after hydrothermal treatment; X-ray powder diffraction patterns of (*1*) anatase, (*2*) zirconium titanate, and (*3*) monoclinic zirconium dioxide form the ICSD database (nos. 82082, 51049, and 68782, respectively); (b) change in the phase composition and (c) crystallite size depending on the hydrothermal treatment duration.

in the fraction of crystalline phases is observed (Figs. 5a, 5b). The size of $Zr_xTi_{(1-x)}O_4$ crystallites does not change, which also indicates the predominance of nucleation processes over crystal growth processes. The average size of m-ZrO_2(sol. sol.) crystallites is 12 ± 5 nm.

An increase in the duration of isothermal treatment to 48 h does not lead to the appearance of peaks of new phases in the diffraction patterns (Fig. 5a). According to XRD data, the fraction of $Zr_xTi_{(1-x)}O_4$ decreases, as does the average size of its crystallites, while the fraction of simple oxides increases (Fig. 5b). The average crystallite size of a-TiO_2(sol. sol.) increases, while the average size of m-ZrO_2(sol. sol.) crystallites does not change.

All the above observations suggest that titanium, which is in excess and not included in the structure of the double hydroxide, crystallizes in the form of a solid solution with the anatase structure; double hydroxide, apparently, has a structure close to the high-temperature disordered $Zr_xTi_{(1-x)}O_4$ phase with the α-PbO_2 structure, and upon long-term isothermal treatment under hydrothermal conditions, it crystallizes in a metastable state in the form of this phase, which, however, with increasing the duration of isothermal treatment, does not undergo ordering and transition to a more stable modification, but undergoes a gradual decomposition into solid solutions based on simple oxides.

CONCLUSIONS

The processes of phase formation in the ZrO_2–TiO_2–H_2O system under hydrothermal isothermal conditions have been comprehensively studied. The

mutual influence of the components of the system on the formation of nanocrystalline simple of titanium oxide (anatase structure) and zirconium oxide (monoclinic and tetragonal structures) and solid solutions based on them has been shown. The formation of a nanocrystalline high-temperature disordered phase of variable composition $Zr_xTi_{(1-x)}O_4$ with scrutinite structure (α-PbO_2) and its limited stability under the considered hydrothermal conditions have been established. It has been demonstrated that the $Zr_xTi_{(1-x)}O_4$ phase decomposes to solid solutions based on titanium dioxide with the anatase structure and monoclinic zirconia, which corresponds to the equilibrium composition of the low-temperature region of the actual phase diagram of the ZrO_2–TiO_2 system.

ACKNOWLEDGMENTS

We are grateful to Corresponding Member of the RAS V.V. Gusarov for the proposed direction for research, attention to the work, and fruitful discussion of the results. We also thank V.I. Al'myashev for help in the study of materials by X-ray electron probe microanalysis.

FUNDING

The work was supported by the Russian Science Foundation, project no. 21-13-00260.

CONFLICT OF INTEREST

The authors declare no conflicts of interest.

AUTHOR CONTRIBUTIONS

A.K. Bachina and O.V. Almjasheva invented and developed the experiment; A.K. Bachina and V.I. Popkov synthesized the samples and carried out their physicochemical analysis; A.K. Bachina and O.V. Almjasheva participated in data processing. All authors participated in the discussion of the results and writing the text of the article.

REFERENCES

1. N. Kumar and G. Irfan, Mater. Today Proc. **38**, 2649 (2020). https://doi.org/10.1016/j.matpr.2020.08.240
2. B. M. Reddy and A. Khan, Catal. Rev. Sci. Eng. **47**, 257 (2005). https://doi.org/10.1081/CR-200057488
3. E. Salahinejad, M. J. Hadianfard, D. D. Macdonald, et al., J. Biomed. Nanotechnol. **9**, 1327 (2013). https://doi.org/10.1166/jbn.2013.1619
4. C. Liu, X. Li, C. Xu, et al., Ceram. Int. **46**, 20943 (2020). https://doi.org/10.1016/j.ceramint.2020.05.152
5. A. Zaleska, Recent Patents Eng. **2**, 157 (2008). https://doi.org/10.2174/187221208786306289
6. R. Daghrir, P. Drogui, and D. Robert, Ind. Eng. Chem. Res. **52**, 3581 (2013). https://doi.org/10.1021/ie303468t
7. J. Chevalier and L. Gremillard, J. Eur. Ceram. Soc. **29**, 1245 (2009). https://doi.org/10.1016/j.jeurceramsoc.2008.08.025
8. V. A. Lebedev, D. A. Kozlov, I. V. Kolesnik, et al., Appl. Catal. B: Environ. **195**, 39 (2016). https://doi.org/10.1016/j.apcatb.2016.05.010
9. Y. Yang, Y.-Hang Cui, L. Miao, et al., Powder Technol. **338**, 304 (2018). https://doi.org/10.1016/j.powtec.2018.07.038
10. M. Mozafari, E. Salahinejad, V. Shabafrooz, et al., Int. J. Nanomed. **8**, 1665 (2013). https://doi.org/10.2147/IJN.S42659
11. D. N. Grishchenko, A. V. Golub, V. G. Kuryavyi, et al., Russ. J. Inorg. Chem. **66**, 1592 (2021). https://doi.org/10.1134/S0036023621100065
12. A. V. Zdravkov, Y. S. Kudryashova, and R. S. Abiev, Russ. J. Gen. Chem. **90**, 1677 (2020). https://doi.org/10.1134/S1070363220090145
13. R. E. Newnham, J. Am. Ceram. Soc. **50**, 216 (1967). https://doi.org/10.1111/j.1151-2916.1967.tb15085.x
14. E. L. Sham, M. A. G. Aranda, E. M. Farfan-Torres, et al., J. Solid State Chem. **139**, 225 (1998). https://doi.org/10.1006/jssc.1998.7833
15. F. H. Brown and P. Duwez, J. Am. Ceram. Soc. **37**, 129 (1954).
16. W. Coughanour, R. S. Roth, and V. A. Deprosse, J. Res. Natl. Bur. Stand **52**, 37 (1954).
17. A. E. McHale and R. S. Roth, J. Am. Ceram. Soc. **69**, 827 (1986).
18. P. Bordet, A. McHale, A. Santoro, et al., J. Solid State Chem. **64**, 30 (1986). https://doi.org/10.1016/0022-4596(86)90119-2
19. U. Troitzsch, A. G. Christy, and D. J. Ellis, J. Am. Ceram. Soc. **87**, 2058 (2005). https://doi.org/10.1111/j.1151-2916.2004.tb06360.x
20. N. Vittayakorn, J. Ceram. Process. Res **7**, 288 (2006).
21. F. Azough, R. Freer, C. L. Wang, et al., J. Mater. Sci. **31**, 2539 (1996). https://doi.org/10.1007/BF00687279
22. S. V. Pol, V. G. Pol, A. Gedanken, et al., J. Phys. Chem. **111**, 2484. https://doi.org/10.1007/BF00687279
23. U. Troitzsch and D. J. Ellis, J. Mater. Sci. **40**, 4571 (2005). https://doi.org/10.1007/s10853-005-1116-7
24. U. Troitzsch, A. G. Christy, and D. J. Ellis, Phys. Chem. Miner. **32**, 504 (2005). https://doi.org/10.1007/s00269-005-0027-0
25. R. Christoffersen and P. K. Davies, J. Am. Ceram. Soc. **75**, 563 (1992). https://doi.org/10.1111/j.1151-2916.1992.tb07843.x
26. L. M. Oanh, D. B. Do, N. M. Hung, et al., J. Electron. Mater. **45**, 2553 (2016). https://doi.org/10.1007/s11664-016-4412-x
27. A.K. Bachina, O.V. Al'myasheva, D.P. Danilovich, et al., Russ. J. Phys. Chem. **95**, 1529 (2021). https://doi.org/10.1134/S0036024421080057

28. U. Troitzsch, A. G. Christy, and D. J. Ellis, J. Solid State Chem. **180**, 2885 (2007). https://doi.org/10.1016/j.jssc.2007.08.020
29. A. Gajovic, A. Santic, I. Djerdj, et al., J. Alloys Compd. **479**, 525 (2009).
30. E. López-López, C. Baudín, R. Moreno, et al., J. Eur. Ceram. Soc. **32**, 299 (2012). https://doi.org/10.1016/j.jeurceramsoc.2011.08.004
31. K. Byrappa and T. Adschiri, Prog. Cryst. Growth Charact. Mater. **53**, 117 (2007). https://doi.org/10.1016/j.pcrysgrow.2007.04.001
32. Yu. V. Kolen'ko, A. A. Burukhin, B. R. Churagulov, et al., Zh. Neorg. Khim. **47**, 1755 (2002).
33. O. V. Almjasheva, Nanosyst. Phys., Chem. Math. **7**, 1031 (2016). https://doi.org/10.17586/2220-8054-2016-7-6-1031-1049
34. R. P. Denkewicz, K. S. TenHuisen, and J. H. Adair, J. Mater. Res. **5**, 2698 (1990). https://doi.org/10.1557/JMR.1990.2698
35. F. Yu. Sharikov, O. V. Almjasheva, and V. V. Gusarov, Russ. J. Inorg. Chem. **51**, 1538 (2006). https://doi.org/10.1134/S0036023606100044
36. O. V. Pozhidaeva, E. N. Korytkova, D. P. Romanov, et al., Zh. Obshch. Khim. **72**, 910 (2002).
37. A. V. Shevchenko, L. M. Lopato, I. M. Maister, et al., Zh. Neorg. Khim. **25**, 1379 (1980).
38. H. Nishizawa and Y. Aoki, J. Solid State Chem. **56**, 158 (1985). https://doi.org/10.1016/0022-4596(85)90052-0
39. Yu. I. Sukharev, V. V. Avdin, A. A. Lymar, et al., J. Struct. Chem. **47**, 151 (2006). https://doi.org/10.1007/s10947-006-0280-1
40. M. Z. C. Hu, J. T. Zielke, J. S. Lin, et al., J. Mater. Res. **14**, 103 (1999). https://doi.org/10.1557/JMR.1999.0017
41. A. K. Bachina, O. V. Almjasheva, V. I. Popkov, et al., J. Cryst. Growth **576**, 126371 (2021). https://doi.org/10.1016/j.jcrysgro.2021.126371
42. A. Vasilevskaya, O. V. Almjasheva, and V. V. Gusarov, J. Nanoparticle Res. **18** (2016). https://doi.org/10.1007/s11051-016-3494-y

Translated by G. Kirakosyan